Relevance of Low-Rm MHD for Surface Viscosimetry of Liquid Metals

K. Patouillet[1,2], L. Davoust[1], O. Doche[1], V. Ebrahimian[2]

[1] SIMaP/EPM, 1340 rue de la piscine, 38402 St. Martin d'Hères, France
[2] Montupet, Techcenter 3 rue de Nogent, 60290 Laigneville, France

kevin.patouillet@simap.grenoble-inp.fr

Abstract
This paper presents a theoretical background which justifies the benefits of MHD using a magnetic field for surface viscosimetry of liquid/melted metals. The system considered is based on an annular shallow-channel layout filled with a melted metal covered by an oxide layer, and pervaded by a uniform static magnetic field. The latter permits to monitor the coupling between surface rheology and a supporting flow due to the well-known 2-D tendency of low-Rm magnetohydrodynamics. The impact of a non-planar interface and/or a non-uniformly oxidized interface can be investigated and the surface viscosity better identified.

Key words: Liquid/melted metal, MHD, Surface viscosimetry, Capillary length, Non-uniform surface viscosity.

Introduction

During casting processes, melted metals tend to oxidize quickly in contact with ambient air. A thin oxide layer of about 1 µm thick develops at the air/metal interface. From a modeling point of view, the oxide layer can be described from a revised boundary condition.
Through the Gibbs approach, the physicochemical parameters of the oxidized surface can be taken into account with a macroscopic point of view. This approach requires the introduction of in-excess quantities assigned to the interface: the surface shear viscosity η_s, the surface dilatational viscosity κ_s and the surface tension γ.
To identify the rheological parameters of the oxidized layer, a surface viscometer is used. The concept is firstly introduced in 1970 by Mannheimer and Schechter [1] and has shown a good sensitivity in an annular deep-channel viscometer. More recently, many authors [2] worked on this kind of configuration to determine the rheological properties of a given fluid covered by a monolayer of surfactants.
The use of MHD surface viscosimetry has been successfully proposed for investigating the case of liquid metals, as the galinstan, covered by a thin oxide layer [3]. Indeed, since the liquid metals are electroconductive, the application of a uniform magnetic field B is relevant for several reasons. It permits to monitor the coupling between the viscous surface and the carrier sub-phase by activating Hartmann layers [4]. Moreover, it promotes the 2-D diffusion of the input shearing from the rotating floor up to the liquid surface, and can promote the magnetic extinction of the swirl component of the centrifugally-induced overturning flow [5]. Thus, for a large enough magnetic field, only the surface shear viscosity governs the behavior of the oxide layer avoiding the classical artifact due to surface dilatation.
In this study, two assumptions usually made in the literature are thrown into question. First, the liquid surface is no more considered as planar, which is particularly required for a capillary length, l_c, as large as the one of aluminum. Second, the radially-inwards oxide packing [6] induced by centrifugation of the underlying bulk, is no more considered negligible since it causes a non-uniform surface viscosity along the oxide layer.

Theoretical ingredients

Geometry:

The system considered is an annular MHD shallow-channel where a fluid is end-driven by a rotating floor at angular speed Ω between an inner side wall (radius $r_i = 3$ cm) and an outer side wall (radius $r_o = 7$ cm). The shape of the surface, no more considered as planar, results from the resolution of Young-Laplace equation expressed in cylindrical coordinate $\{O, \boldsymbol{e_r}, \boldsymbol{e_\theta}, \boldsymbol{e_z}\}$,

$$\frac{1}{(1+h'^2)^{3/2}}\left(h'' + \frac{h'}{r} + \frac{h'^3}{r}\right) = \frac{h}{l_c^2}, \tag{1}$$

where h' and h'' are respectively the first and the second radial derivatives of the height h. The capillary length l_c is defined from the surface tension γ, the density ρ and the acceleration of gravity g:

$$l_c^2 = \frac{\gamma}{\rho g}. \tag{2}$$

The wetting angle β is imposed on both walls through the following Neumann boundary condition:

$$h' = -\coth\beta\,. \tag{3}$$

For this special layout, the average liquid depth, h_0, is chosen as small as possible compared to the radial gap of the

channel. In other word, the depth-to-width ratio, ε, is much smaller than unity. Indeed, it can be demonstrated that it tends to magnify the coupling terms between surface and subphase flows due to stronger velocity gradients involved along the vertical direction.

Bulk flow:

The annular MHD flow is supposed to be axisymmetric, permanent, laminar, and incompressible. The fluid is Newtonian and electroconductive with a dynamic viscosity η and an electric conductivity σ. The conventional dimensionless number governing the bulk flow dynamics, the Reynolds and the Hartmann numbers, are respectively defined by:

$$Re = \frac{\rho \Omega r_o^2}{\eta}, \qquad Ha = Br_o\sqrt{\sigma/\eta}. \tag{4}$$

As usual in MHD of liquid metals, the magnetic Reynolds number is small so that the imposed magnetic field is not convected by the annular flow. The weakly coupled MHD model is then formulated with the following electromotive density current $\boldsymbol{j}$ and Lorentz force $\boldsymbol{F}$:

$$\boldsymbol{j} = \sigma(-\boldsymbol{\nabla}\phi + \boldsymbol{v} \times \boldsymbol{B}), \qquad \boldsymbol{F} = \boldsymbol{j} \times \boldsymbol{B}, \tag{5}$$

where ϕ is the electric potential, $\boldsymbol{v}$ is the velocity field and $\boldsymbol{B}$ is the magnetic field approximated by:

$$\boldsymbol{B} = B\boldsymbol{e_z}. \tag{6}$$

The electromagnetic part is described by a formulation based on Maxwell equations and the continuity equation for the total magnetic field, completed by the generalized Ohm's law. The flow is governed by Navier-Stokes equations with the Lorentz force as a body force.

The boundary conditions are summarized in Fig. 1. The constant vertical magnetic field is imposed in the surrounding atmosphere with an electrical insulation at the melted metal boundaries. No-slip boundary conditions are applied at the outer and inner walls together with lubrication conditions in the gaps of δ thickness. Finally, the boundary condition at the liquid/gas interface is found by solving surface rheology equations in next section.

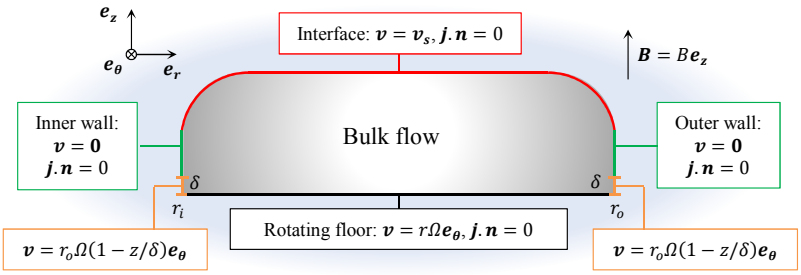

Fig. 1: Geometry and boundary conditions of the channel cross section

Surface flow:

Concerning the mechanics of the oxidized interface, as previously mentioned, the macroscopic point of view is adopted with a zero-thickness interface. This leads to the introduction of a (in-excess) surface stress tensor $\bar{\bar{T}}_s$ linearly related to a (in-excess) surface rate-of-deformation tensor (Boussinesq-Scriven law):

$$\bar{\bar{T}}_s = [\gamma + (\kappa_s - \eta_s)\boldsymbol{\nabla_s}.\boldsymbol{v_s}]\bar{\bar{P}}_s + \eta_s\left[\bar{\bar{P}}_s.(\boldsymbol{\nabla_s}\boldsymbol{v_s}) + (\boldsymbol{\nabla_s}\boldsymbol{v_s})^t.\bar{\bar{P}}_s\right]. \tag{7}$$

The surface projection tensor $\bar{\bar{P}}_s$ is defined from normal unit vector, $\boldsymbol{n}$, and the "s" subscript refers to the variables at the surface. This law involves the three rheological parameters $(\gamma, \eta_s, \kappa_s)$, each of them involves the following dimensionless numbers: the Marangoni number, the surface shear and surface dilatational Boussinesq numbers :

$$Ma = \varepsilon\frac{\gamma}{r_o\eta\Omega}, \qquad Bo_{\eta s} = \varepsilon\frac{\eta_s}{r_o\eta}, \qquad Bo_{\kappa s} = \varepsilon\frac{\kappa_s}{r_o\eta}. \tag{8}$$

It is assumed that these quantities depend on the level of oxidation, which itself is related to the oxygen rate of the surrounding atmosphere. The governing equation of surface mechanics is a jump momentum balance (JMB) derived from an elementary volume straddling the liquid surface. With no surface body force, the JMB writes according to a balance between the surface stresses and the jump in bulk stresses normally applied on both sides of the oxide layer [7]:

$$\boldsymbol{\nabla_s}.\bar{\bar{T}}_s = [\![\bar{\bar{T}}.\boldsymbol{n}]\!]. \tag{9}$$

Magnetic damping:

If the following condition is satisfied,

$$\frac{Ha}{\sqrt{Re}}\frac{r_o}{h_0} \gg 1, \tag{10}$$

the swirl component of the centrifugally-induced overturning flow is damped [3], and the MHD flow is purely 2D-azimuthal. Therefore, the surface shear viscosity can be selectively studied, since the surface dilatational viscosity is no longer solicited without any significant radial component of the surface flow. The eventual residual impact of a radially-inwards oxide packing can be taken into account through a non-uniform surface shear viscosity.

Under these conditions, the dimensionless azimuthal component of the JMB can be explicitly written as:

$$\underbrace{Bo_{\eta s}\frac{\partial}{\partial s^*}\left(\frac{1}{r^*}\frac{\partial}{\partial s^*}\left(r^* v_{\theta s}^*\right)\right)}_{\text{2-D viscous shear}} + \underbrace{\frac{\partial Bo_{\eta s}}{\partial s^*}\left(r^*\frac{\partial}{\partial s^*}\left(\frac{v_{\theta s}^*}{r^*}\right)\right)}_{\text{2-D non-uniformity in shear visosity}} + \underbrace{Bo_{\eta s}\frac{v_{\theta s}^*}{r^*}\frac{2\varepsilon^2 \mathrm{h}'^* \mathrm{h}''^*}{\left(1+\varepsilon^2 \mathrm{h}'^{*2}\right)^2}}_{\text{Surface curvature}} = \underbrace{r^*\frac{\partial}{\partial n^*}\left(\frac{v_\theta^*}{r^*}\right)}_{\text{Liquid shear from underlying sub-phase}}, \tag{11}$$

where the dimensionless tangential and normal derivatives are respectively defined by:

$$\frac{\partial .}{\partial s^*} = \frac{1}{\sqrt{1+\varepsilon^2 \mathrm{h}'^{*2}}}\left(\frac{\partial .}{\partial r^*} + \mathrm{h}'^*\frac{\partial .}{\partial z^*}\right), \quad \frac{\partial .}{\partial n^*} = \frac{1}{\sqrt{1+\varepsilon^2 \mathrm{h}'^{*2}}}\left(\frac{\partial .}{\partial z^*} - \varepsilon^2 \mathrm{h}'^*\frac{\partial .}{\partial r^*}\right). \tag{12}$$

It is worthy to note that the normal component of the JMB is nothing but the Young-Laplace equation.

Surface shear viscosity model

The radially-inwards oxide packing leads to a non-uniform surface shear viscosity. Then, the Boussinesq number $Bo_{\eta s}$ is defined along the dimensionless curvilinear abscissa, s^*, according to the model proposed in [6]:

$$Bo_{\eta s}(s^*) = Bo_m\left(1 + \frac{1-R}{1+R}\tanh\left(\frac{s^* - s_f^*}{\delta_f^*}\right)\right). \tag{13}$$

The latter involves the median Boussinesq number Bo_m, the location of the segregation front s_f^*, the thickness of the segregation front δ_f^*, and the ratio R between the inner and outer Boussinesq numbers. All these quantities are normalized by the radial extent of the liquid/gas interface or by the average liquid depth .

Results and interpretations

Numerical simulations are performed with Comsol Multiphysics which is a software based on finite element method. A fully-coupled approach is solved with a linear stationary direct solver (MUMPS). The internal mathematical functions are used to model the bulk MHD flow and weak formulations for surface equations (azimuthal JMB and Young-Laplace equations). The mesh is composed of triangular elements with a rectangular boundary layer mesh at the walls.

With a planar interface and uniform surface properties, a good agreement is found between this numerical model and existing analytical results for MHD flow [4]. The hydrodynamic flow with a radially-dependent surface shear viscosity is also well validated based on an asymptotic analytical model [6].

Physical properties of pure aluminum at 973 K, used in numerical simulations, are summarized in Tab. 1.

ρ [kg. m^{-3}]	η [Pa. s]	σ [Ω^{-1}. m^{-1}]	γ [N. m^{-1}]	l_c [m]
2357	1.286×10^{-3}	4.034×10^{6}	0.703	5.514×10^{-3}

Tab. 1: Physical properties of aluminum at 973 K used for numerical simulations

First results presented in this study are dedicated to surface velocity profiles. It can be seen that the impact of the wetting angle is significant close to the side walls and that the tangential surface shear tends to increase with the wetting angle (see Fig. 2). Indeed, a dead zone arises near the side walls for the wetting case, which causes a decrease in the surface velocity, while the bulk flow drives the side parts of the oxide layer for the non-wetting case. These effects are weakened for a high Hartman number due to the 2-D tendency.

Typical Boussinesq profiles used to evaluate the impact of the radially-inwards oxide packing are shown in Fig. 4. Surface velocity profiles are mainly affected at the outer part of the viscometer where a bump is created (Fig. 3 and 5). As expected, a higher jump between the inner and outer Boussinesq numbers, which can be obtained with a larger median Boussinesq number Bo_m or Boussinesq ratio R, leads to greater effects. As previously, the impact of a non-uniform contamination along the surface is reduced for a large enough Hartmann number.

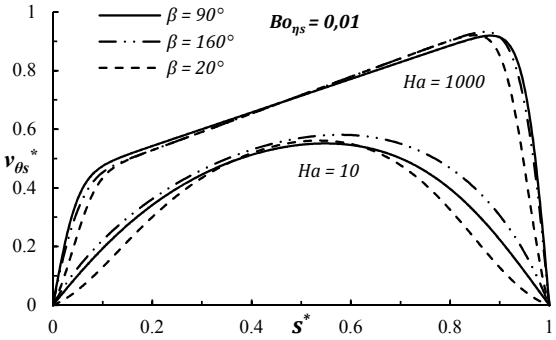

Fig. 2: $v^*_{\theta s}$ profiles for $R = 1$ and $Bo_m = 0.01$.

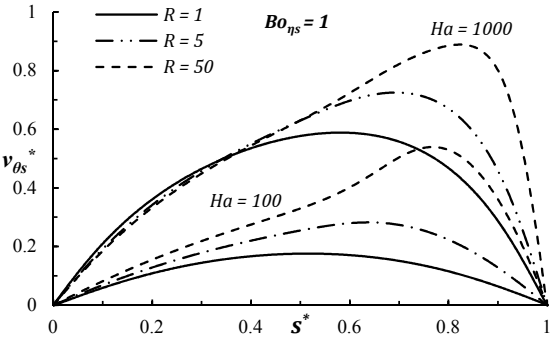

Fig. 3: $v^*_{\theta s}$ profiles for $\beta = 160°$ and $Bo_m = 1$.

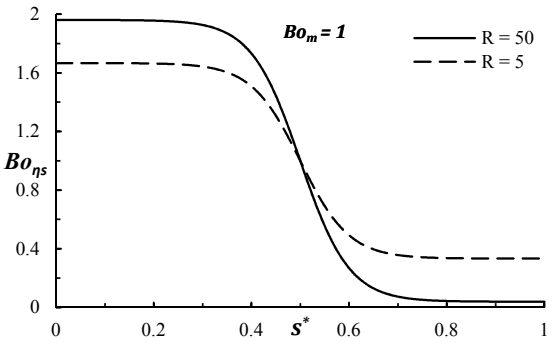

Fig. 4: $Bo_{\eta s}$ profiles for $Bo_m = 1$, $s^*_f = 0.5$ and $\delta^*_f = 0.1$.

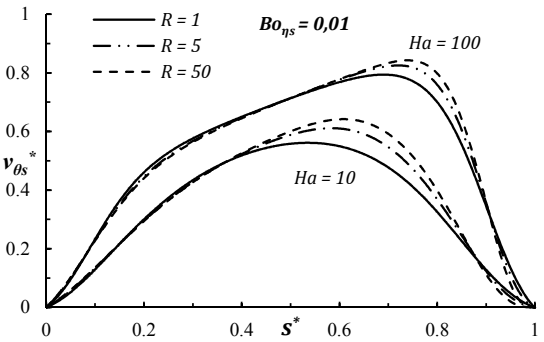

Fig. 5: $v^*_{\theta s}$ profiles for $\beta = 20°$ and $Bo_m = 0.01$.

Thus, the magnetic field can be helpful to detect the possible presence of defects usually neglected, due to the 2-D tendency. However, the surface shear stress and the bulk shear stress at the interface corrected by the magnetic effects should be balanced.

To compare these quantities, a revised Boussinesq number [4] is introduced:

$$\widetilde{Bo}_{\eta s} = \frac{2\,Bo_m}{\varepsilon^3 Ha\big(1+\exp(-\varepsilon Ha)\big)}. \tag{14}$$

For a Hartmann number significantly larger than the Boussinesq number, the surface velocity is almost perfectly aligned with the rotating floor, whatever the interface shape or the surface viscosity profile. In other word, a revised Boussinesq number smaller than unity does not allow surface flow to be sensitive to the wetting effect or to surface viscosity non-uniformities.

Conclusion

By comparing the experimental surface velocity field along an oxide layer with numerical simulations presented in this study, it is now possible to evaluate the surface physicochemical parameters of oxidized melted metals with a better accuracy. Indeed, artifacts due to the wetting effect and to surface viscosity non-uniformities are taken into account as long as the revised Boussinesq number is greater than or equal to unity.

Acknowledgments

The authors are grateful to C. Bozonnet for his contribution to modeling during his master thesis. The laboratory SIMaP is part of the LabEx Tec 21 (Investissements d'avenenir - Grant Agreement No. ANR-11-LABX-0030).

References

1. R.J. Mannheimer & R.S. Schechter, *J. Fluid Mech*, **470** (2002) 135-149
2. J.M. Lopez, R. Miraghaie & A.H. Hirsa, *J. Colloid Interf. Sci.* **248**:1, (2002) 103-110
3. J. Delacroix, L. Davoust & K. Patouillet, *Rev. Sci. Instrum.* **89**:1 (2018) 015103
4. J. Delacroix & L. Davoust, *Phys. Fluids*, **26**:3 (2014) 037102
5. J. Delacroix & L. Davoust, *Phys. Fluids*, **27**:6 (2015) 062104
6. L. Davoust, Y.L. Huang, S.H. Chang, Surface Science, **603**:17 (2009) 2777-2788
7. J.C. Slattery, L. Sagis, & E. Oh, New York: Springer-Verlag, (2007) 22,360,712.